

Sorption and Surface Chemistry of Aminoethanol and Ethanediamine on H-Mordenites

Gerhard D. Pirngruber, Gabriele Eder-Mirth, and Johannes A. Lercher*

University of Twente, Department of Chemical Technology, P.O. Box 217, 7500 AE Enschede, The Netherlands

Received: May 23, 1996; In Final Form: October 21, 1996[®]

The sorption and surface chemistry of 2-aminoethanol and 1,2-ethanediamine on acidic mordenites was studied in situ by means of IR spectroscopy. Upon sorption on the hydroxyl groups of the zeolite, the amino group of aminoethanol and one amino group of ethanediamine is protonated. The extent of interaction of the second functional group with the zeolite decreases with increasing Si/Al ratio. On mordenites with a high acid site density the OH group of aminoethanol was strongly hydrogen bonded to the zeolite, while this interaction was less pronounced in the samples with a low site density. For ethanediamine sorbed on mordenites with a high acid site density the fraction of double-protonated molecules was higher than for samples with a low aluminum content. When aminoethanol and ammonia were coadsorbed on Si-rich mordenite with a large-pore volume, aminoethanol was preferentially adsorbed. On Al-rich samples with a small pore volume, the formation of a coadsorption complex is indicated in which aminoethanol and ammonia are sorbed on neighboring acid sites and interact via hydrogen bonding. During TPD of aminoethanol from H-mordenites, the molecule eliminated water at approximately 600 K. The formed intermediate decomposed further into ammonia and hydrocarbons. During TPD of ethanediamine from H-mordenites, the desorption of more weakly bound species and the increased mobility at higher temperatures enabled all ethanediamine molecules to be protonated on both amino groups. The double protonated species then desorbed at temperatures above 600 K upon decomposition into ammonia and hydrocarbons.

1. Introduction

1,2-Ethanediamine (ethylenediamine, EDA) is an important organic intermediate for products in a wide variety of applications^{1,2} such as production of EDTA, fungicides, bleach activators, polyamides, etc. Currently, two major processes are used for production of ethanediamine, i.e., the ethylene dichloride process and the reductive amination of aminoethanol. In the ethylene dichloride process^{1,2} 1,2-dichloroethane (ethylene dichloride) is converted with an aqueous ammonia solution to EDA and higher amines. Large amounts of sodium chloride are produced as a byproduct. The reductive amination^{1,2} of 2-aminoethanol (ethanolamine, AE) is more selective but requires the use of high pressures (around 200 bar).

Due to these disadvantages of the currently used production processes, there is rising interest in an acid-catalyzed conversion of aminoethanol and ammonia to ethanediamine at ambient pressure. Preliminary studies showed mordenite to be the most promising catalyst for this reaction.^{3,4} To arrive at a more detailed understanding of the surface chemistry involved in the conversion of AE to EDA over mordenite catalysts, the sorption and temperature-programmed desorption of the reactants (AE and ammonia) and the product (EDA) were studied on parent and postsynthesis modified mordenites.

2. Experimental Section

Catalysts. Synthetic, ammonium-exchanged mordenites (provided by the Catalysis Society of Japan) with a SiO₂/Al₂O₃ ratio of 10 (HM10) and 20 (HM20) were used. Since the sample HM10 contained extralattice material, an EDTA-leached material was prepared.⁵ For that purpose the sodium form of mordenite M10 (SiO₂/Al₂O₃ = 10) was refluxed in an aqueous 0.01 M EDTA solution for 16 h. After filtering and drying, a 3-fold ion exchange was performed with a 1 M NH₄NO₃ solution. The resulting material will be referred to as EDTA-HM10.

The BET surface area and the micropore volume of all catalysts were measured on an accelerated surface area porosimeter equipment (ASAP 2400). The amount of extraframework alumina (EFAL) was determined as the amount of octahedrally coordinated aluminium detected by ²⁷Al MAS NMR. The concentration of strong Brønsted acid sites was calculated from the amount of ammonia that remained adsorbed on the zeolite after evacuation at 373 K for 10 h (at a pressure of 10⁻⁶ mbar). This procedure ensured complete removal of all physisorbed species. These physicochemical properties of the samples are summarized in Table 1 (compare also the values reported by Sawa et al.⁶).

FTIR Measurements. For the infrared spectroscopic measurements approximately 5 mg of the material were pressed into a self-supporting wafer and placed into a vacuum chamber⁷ equipped with infrared transparent windows (base pressure <10⁻⁶ mbar). The mordenites were heated to 873 K with a temperature increment of 10 K min⁻¹ and kept at this temperature for 3–4 h in order to convert them into the protonic form. Adsorption was carried out at 323 K starting at a partial pressure of 10⁻³ mbar. After equilibration under these conditions, the partial pressure was raised to 10⁻¹ mbar. The adsorption process was followed in situ by time-resolved IR spectroscopy.

For the coadsorption experiments, the zeolite was first equilibrated with 10⁻³ mbar of the first substance. Then, the second substance was admitted with a pressure of 10⁻³ mbar, while keeping the partial pressure of the first adsorbate constant.

After the sorption experiments the sample chamber was evacuated for 90 min, and temperature-programmed desorption (TPD) was carried out with a temperature increment of 5 K min⁻¹. IR spectra were recorded every 10–20 K. The gas phase was simultaneously analyzed by mass spectrometry (Balzers QMG 311). The IR spectra were recorded with a Bruker IFS 88 FTIR spectrometer (30 scans, resolution 4 cm⁻¹) in the transmission-adsorption mode. All treatments (activation, adsorption, and TPD) were monitored in situ. A spectrum

[®] Abstract published in *Advance ACS Abstracts*, December 15, 1996.

TABLE 1: Physicochemical Properties of the Investigated Mordenites

catalyst	microporous vol ^a (cm ³ /g)	Si/Al	EFAL (%)	Brønsted acid sites (mmol/g)	
				exp ^b	theor ^c
HM20	0.13 ± 0.01	10	<1	1.3	1.5
EDTA-HM10	0.13 ± 0.02	6	nd ^e	1.9	2.4 ^d
HM10	0.05	5	8	2.1	2.8

^a Calculated from the slope of the *t*-plot in the range *t* = 3.5–5 Å.

^b Determined as amount of irreversibly adsorbed ammonia. ^c As calculated from the framework Si/Al ratio. ^d As calculated from the Si/Al-ratio. ^e Not determined.

of the empty, evacuated IR cell was used as reference (*I*₀) to convert the single-beam spectra (*I*) into absorbance spectral (log *I*₀/*I*). The latter were baseline corrected in the region from 3800 to 1300 cm⁻¹. To correct for the varying sample thickness of the different wafers, the integral intensity of the overtones of the lattice vibrational bands at 1975 and 1870 cm⁻¹ was used to normalize the intensities of all spectra.

For illustration of the changes occurring upon adsorption, the difference spectra between the sample equilibrated with the adsorbate at a given partial pressure and the sample in the activated state are reported here. In that representation bands pointing downward correspond to a decrease in intensity after admission of the adsorbate, while bands pointing upward indicate an increase.

Temperature-Programmed Desorption (TPD). Because of the limited sensitivity of the mass spectrometric signals during TPD in the IR cell, the experiments were repeated in a vacuum TPD apparatus.⁸ Samples were activated for 1 h at 823 K (base pressure ~10⁻³ mbar). Adsorption was then carried out at 308 K and partial pressures ranging from 0.5 to 5 mbar. After evacuation at 373 K for 1 h, TPD was performed with a temperature increment of 10 K min⁻¹. The desorbing gas stream was analyzed with a Balzers QMG 420 mass spectrometer.

3. Results

Adsorption of Aminoethanol (AE). The difference spectra between the zeolites in contact with 10⁻³ mbar AE and the activated zeolites are compiled in Figure 1. Table 2 gives an assignment of the most important IR bands.

The negative band at 3610 cm⁻¹ corresponds to a decrease in intensity of the ν_{OH} band of the Brønsted acidic hydroxyl groups caused by an interaction with AE. From this decrease in intensity and the appearance of two bands at 1505 and 1610 cm⁻¹ (characteristic for the symmetric and asymmetric deformation vibrations of NH₃⁺ groups,⁹ whereas only one band at around 1600 cm⁻¹ is expected for a nonprotonated NH₂ group), we conclude that the amino-group of AE was protonated on Brønsted acid sites. The IR spectra (see Figure 2) show that on HM20 and on EDTA-HM10 the ν_{OH} band of the Brønsted OH groups at 3610 cm⁻¹ disappeared completely, while on HM10 20 ± 5% of the Brønsted acidic OH groups remained unperturbed.

The IR band of the OH group of aminoethanol (see Figure 2) was significantly different for aminoethanol sorbed on the three mordenite samples. For AE sorbed on HM10 and on EDTA-HM10 a broad ν_{OH} band between 3600 and 3350 cm⁻¹ was observed. Because of its width and its rather low wavenumber, the band was assigned to hydrogen bridge bonded OH groups. Upon sorption on HM20, however, an additional sharp ν_{OH} band appeared at 3575 cm⁻¹. This band was assigned to weakly bound OH groups as the ν_{OH} band of AE in the gas phase¹⁰ lies at 3671 cm⁻¹.

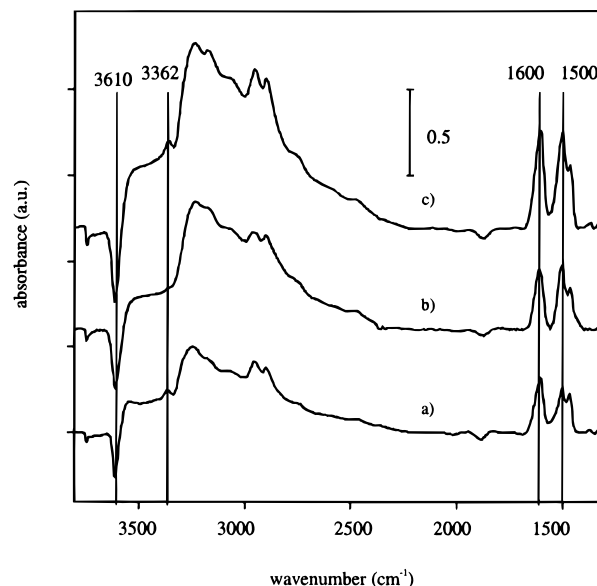


Figure 1. Differences between the IR spectra of HM20 (a), HM10 (b), and EDTA-HM10 (c) equilibrated with 10⁻³ mbar of AE and the spectra of the activated mordenites at 323 K.

TABLE 2: Assignments of the IR Bands of AE Sorbed on HM20, EDTA-HM10, and HM10 at 10⁻³ mbar and 323 K

IR bands (cm ⁻¹) of AE adsorbed on			assignment of the vibration
HM20	EDTA-HM10	HM10	
3575			ν _{OH}
~3500	~3500	~3500	ν _{OH}
3362	3362		ν _{NH₂}
3245, ~3180	3235, ~3175	3233, ~3175,	ν _{NH₃⁺}
~3085	~3075	~3075	
2951, 2894	2951, 2895	2954, 2897	ν _{CH₂}
1601	1603	1610	δ _{NH₃⁺, asym} + δ _{NH₂}
1502	1502	1505	δ _{NH₃⁺, sym}
1462	1461	1460	δ _{CH₂}
1325	1325	1325	δ _{COH}

The small band at 3362 cm⁻¹ and a very weak shoulder at approximately 3300 cm⁻¹ originate from the asymmetric and symmetric stretching vibrations of rather freely vibrating NH₂ groups, respectively. These bands were only observed upon sorption of AE on HM20 and on EDTA-HM10 (see Figure 1).

Upon raising the partial pressure of AE to 10⁻¹ mbar the coverage of the Brønsted sites was increased on HM10, but qualitative changes were not observed in the spectrum. For HM20 the difference between the spectra recorded after equilibration of the zeolite with 10⁻¹ and 10⁻³ mbar of AE is shown in Figure 3. The most prominent features of this difference spectrum are the ν_{OH} band at 3575 cm⁻¹, the asymmetric and symmetric NH₂ stretching vibration bands at 3370 and 3310 cm⁻¹ and the corresponding δ_{NH₂} band at 1598 cm⁻¹. In both cases, i.e., on HM10 and on HM20, most of the changes, induced by increasing the partial pressure to 10⁻¹ mbar were shown to be reversible by evacuation for a few hours. Thus, the above-mentioned bands are assigned to weakly bound (physisorbed) species in the pores of the zeolite.¹¹

Adsorption of Ammonia. The IR spectrum of HM10 equilibrated with 10⁻³ mbar ammonia (see Figure 4b) exhibits bands characteristic for ammonium ions sorbed on the Brønsted acidic sites.¹² The absorbances at 3373, 3265, and 3040 cm⁻¹ were assigned to the N–H stretching vibrations, the band at 1450 cm⁻¹ to N–H deformation vibrations. Recent theoretical calculations showed that NH₄⁺ sorption complexes having two or three hydrogen atoms of the ammonium ions directed toward the lattice oxygen atoms are energetically most favourable.¹³

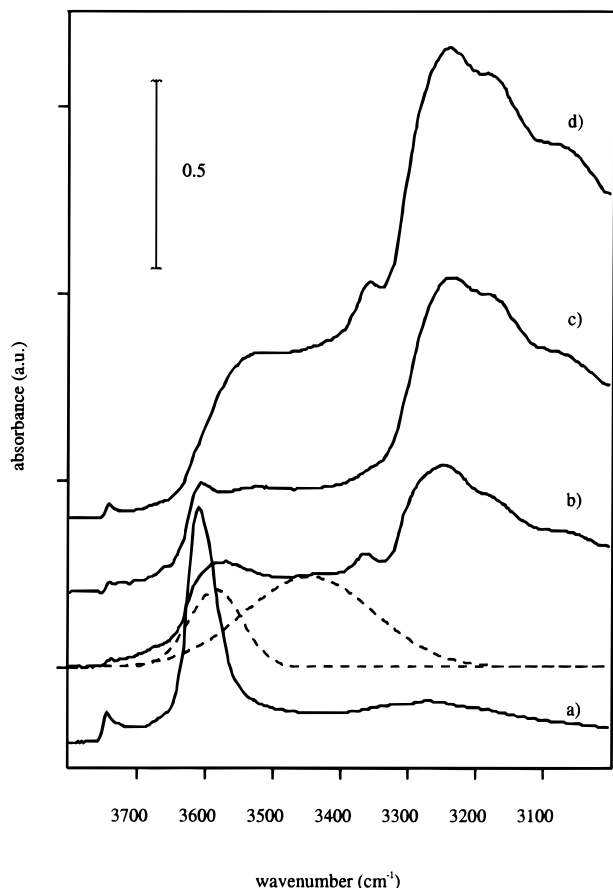


Figure 2. (a) IR spectrum of activated HM10 at 323 K. IR spectra of HM20 (b), HM10 (c), and EDTA-HM10 (d) equilibrated with 10⁻³ mbar of AE at 323 K.

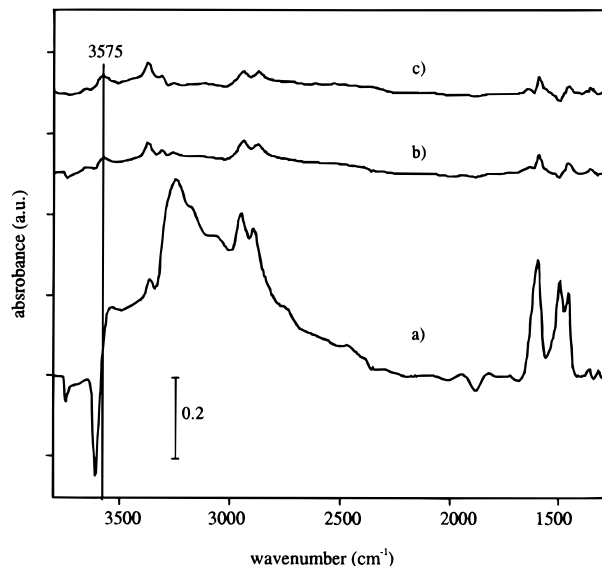


Figure 3. (a) Difference between the IR spectrum of HM20 equilibrated with 10⁻³ mbar AE and the spectrum of the activated mordenite at 323 K. (b) Difference between the IR spectra of HM20 equilibrated with 10⁻¹ and 10⁻³ mbar AE. (c) Difference between the IR spectrum of HM20 equilibrated with 10⁻¹ mbar AE and the spectrum recorded after 1 h of subsequent evacuation.

The band at 3373 cm⁻¹ was, thus, assigned to the relatively free vibrating NH group pointing away from the zeolite pore wall.

Coadsorption of Aminoethanol and Ammonia. When coadsorbed on HM20, the stronger base AE fully replaced ammonia sorbed on the strong Brønsted acid sites. The

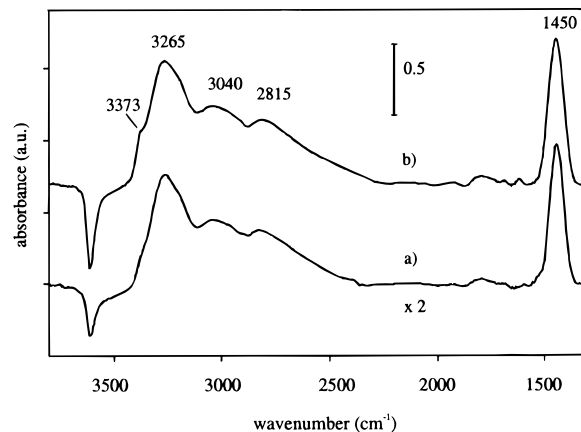


Figure 4. (a) Difference between the IR spectra of HM10 recorded after coadsorption of 10⁻³ mbar ammonia and 10⁻³ mbar AE and after adsorption of 10⁻³ mbar AE alone (at 323 K). (b) Difference between the IR spectrum of HM10 equilibrated with 10⁻³ mbar of ammonia and the spectrum of activated HM10 at 323 K.

spectrum obtained after equilibration with both substances looked almost identical to the spectrum of pure AE at the same partial pressure. Identical IR spectra were obtained regardless of the sequence of adsorption.

On HM10, however, AE could not fully replace preadsorbed ammonia from all Brønsted acid sites, even after coadsorption for 12 h. A detailed spectral fitting indicated that approximately 70% of the ammonia remained sorbed on the acidic hydroxyl groups. In a second experiment the adsorption sequence was reversed and ammonia was cofed as the second reactant. Figure 4 compares the difference between the spectrum recorded after coadsorption of AE and ammonia and that measured after adsorption of AE alone (Figure 4a) and the spectrum of pure ammonia sorbed on HM10 (Figure 4b). The spectrum showing the changes caused by coadsorption was nearly identical with the spectrum of sorbed pure ammonia. Negative bands that could be attributed to a removal of AE from the sorption sites were not observed. The spectrum suggests that the cofed ammonia was sorbed on those Brønsted acid sites that did not interact with AE, as for AE only a coverage of approximately 80% of Brønsted acid sites could be achieved.

However, the relative intensity of the negative band at 3610 cm⁻¹ and the $\delta_{\text{NH}_4^+}$ band at 1450 cm⁻¹ did not match in the spectra of adsorbed (Figure 4b) and coadsorbed ammonia (Figure 4a). Only 20% of the Brønsted acidic sites were additionally covered upon coadsorption of ammonia, but the intensity of the $\delta_{\text{NH}_4^+}$ band at 1450 cm⁻¹ amounted to 45% of the value obtained in the spectrum of pure ammonia. If the absorption coefficient of ammonia does not change upon coadsorption of AE (for coadsorption of methanol and ammonia¹² it was possible to show that the absorption coefficient indeed remains constant), this means that more ammonium ions were sorbed than free acid sites were available, although AE was not replaced from the zeolite. This suggests (see Figure 5) that before admission of ammonia, some Brønsted acid sites interact with the OH group of AE adsorbed via the NH₂ group on a neighboring acid site. Upon coadsorption of ammonia, however, ammonia displaces the hydroxyl group from these acid sites, because protonation of ammonia is energetically more favorable than the hydrogen bridge bond to the OH group of AE.

Another subtle difference in the spectrum of coadsorbed compared to adsorbed ammonia alone was that the intensity of the band at 3373 cm⁻¹ (ν_{NH} of freely vibrating NH groups) was much smaller. This was explained by assuming that the OH

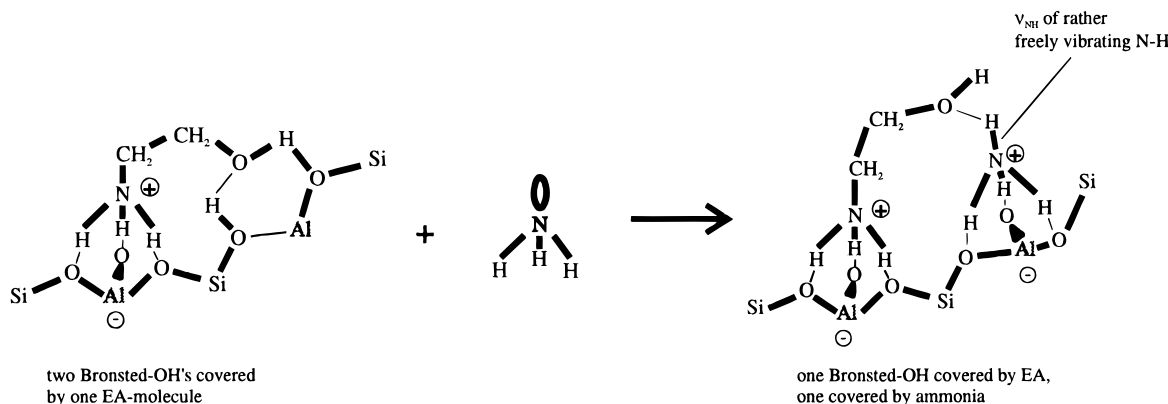


Figure 5. Schematic representation of the coadsorption of AE and ammonia on HM10.

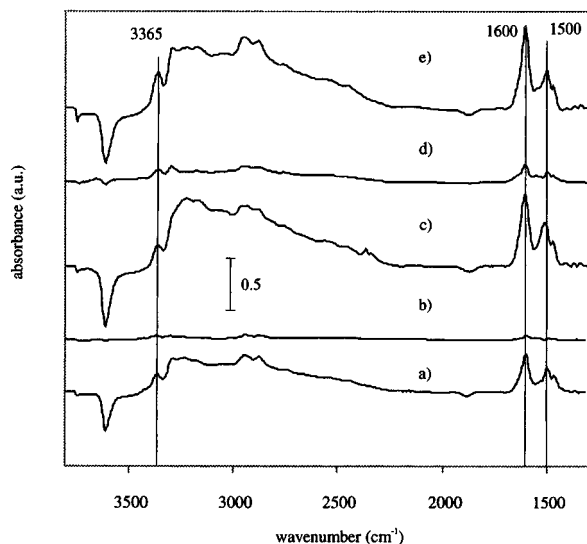


Figure 6. Differences between the IR spectra of HM20 (a), HM10 (c), and EDTA-HM10 (e) equilibrated with 10^{-3} mbar of EDA and the spectra of the activated mordenites at 323 K; difference between the IR spectra of HM20 (b) and HM10 (d) equilibrated with 10^{-1} and with 10^{-3} mbar EDA.

group of AE was hydrogen bridge bonded to the ammonium ion (see Figure 5), thereby causing the band of the freely vibrating NH groups to shift to lower wavenumbers. A similar type of interaction between ammonium ions and OH groups of an alcohol was proposed for the coadsorption of methanol and ammonia on H-mordenites.¹²

It is emphasized again that the obtained results depended on the adsorption sequence, i.e., if ammonia or AE were adsorbed first. The ammonia coverage was roughly 70% for the case where ammonia was adsorbed first and 45% ammonia for the other adsorption sequence (the rest corresponding to AE).

Adsorption of Ethanediamine. The difference spectra obtained upon sorption of 10^{-3} mbar of ethanediamine (EDA) on HM10, EDTA-HM10, and HM20 are compiled in Figure 6. Table 3 lists the assignment of the most important bands.

The appearance of the negative band at 3610 cm^{-1} (indicating a decrease in intensity of the Brønsted acidic OH groups of the zeolite) and two positive bands around 1600 and 1500 cm^{-1} , attributed to the deformation vibrations of a NH_3^+ group (see Figure 6a,c,e), indicated that the amino group(s) of EDA was (were) protonated on the Brønsted acid sites. On HM20 and on EDTA-HM10, the band of the stretching vibration of the Brønsted OH groups at 3610 cm^{-1} disappeared almost completely, whereas on HM10 it retained 10–15% of its intensity.

On all three zeolites sorption of EDA caused the appearance of a band around 3363 cm^{-1} , which was attributed to the

TABLE 3: Assignments of the IR Bands of EDA Sorbed on HM20, EDTA-HM10, and HM10 at 10^{-3} mbar and 323 K

IR bands (cm^{-1}) of EDA on			assignment
HM20	EDTA-HM10	HM10	
3363, 3292	3364, 3292	3361, 3296	ν_{NH_2}
3235, ~ 3175 , ~ 3025	3225, ~ 3175 , ~ 3050	3223, ~ 3170 , ~ 3070	$\nu_{\text{NH}_3^+}$
2945	2950, ~ 2930	2958, ~ 2930	ν_{CH_2}
2876	2895, 2875	2902, 2880	ν_{CH_2}
1603	1603	1604	$\delta_{\text{asym}, \text{NH}_3^+} + \delta_{\text{NH}_2}$
1499	1500	1510	$\delta_{\text{sym}, \text{NH}_3^+}$
1467	1470	1471, 1460	δ_{CH_2}

asymmetric stretching vibration of NH_2 groups. Thus, we conclude that not all amino groups of the sorbed EDA molecules were protonated upon sorption. Upon increasing the partial pressure to 10^{-1} mbar (see Figure 6b,d), mainly the intensity of the bands affiliated with these nonprotonated amino groups increased.

Temperature-Programmed Desorption of Aminoethanol.

Figure 7 compiles the rates of desorption of several characteristic products evolving during TPD. Table 4 compiles the temperatures of the desorption maxima. During TPD of AE from HM10 all sorbed molecules decomposed. Water, hydrocarbons (mainly ethene and propene, but also small amounts of fragments with a molecular weight exceeding that of AE) and ammonia were released from the catalyst, in the sequence given.

During TPD of AE from HM20, molecular desorption of AE was observed at low temperatures (532 K), indicating that these molecules were not very strongly bonded. At higher temperatures AE desorbed reactively, like from HM10. The desorption of water, ethene, and ammonia was similar on HM10 and HM20; however, on HM20 an additional maximum of desorbing ammonia appeared at 673 K.

The TPD experiments performed in the infrared cell yielded qualitatively the same desorption curves. The corresponding infrared spectra recorded during TPD of AE from HM10 are shown in Figure 8. In the temperature region between 500 and 800 K the intensities of the broad band between 3600 and 3350 cm^{-1} (ν_{OH} of AE) and of the band at 1325 cm^{-1} (δ_{OH}) was decreased. The spectra changes were paralleled by the desorption of water.

Around 615 K new bands at 1361 and at 1455 cm^{-1} (attributed to CH_2 deformation vibrations) appeared in the IR spectrum. These bands reached their maximum intensity approximately at 670 K and vanished at higher temperatures. They were attributed to an intermediate species formed from AE by elimination of water. In parallel to the increase in intensity of the bands characteristic for the intermediate, the intensity of the two $\nu_{\text{NH}_3^+}$ bands decreased, and a band appeared

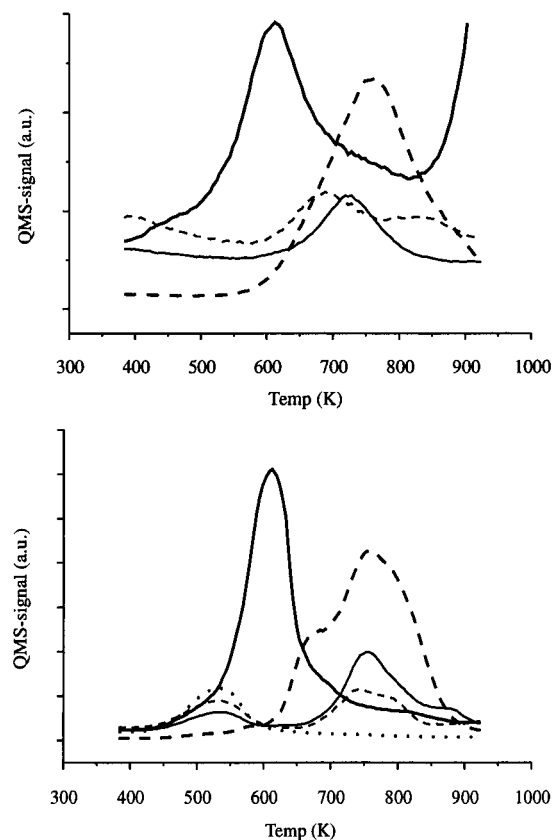


Figure 7. TPD of AE from HM10 (a) and HM20 (b): QMS-signals of mass 16 (NH_3 — · —), mass 18 (H_2O , —), mass 28 (C_2H_4 , —), mass 30 (AE, ···) and mass 43 (C_3H_6 , - - -, $\times 5$).

TABLE 4: Temperature Maxima in the Desorption Rate during TPD of AE from HM10 and HM20

temp (K)		assignment
HM10	HM20	
	532	AE
611	614	H_2O
	673	NH_3
723	756	C_2H_4
757	756	NH_3

at approximately 1450 cm^{-1} , attributed to the deformation vibration of protonated ammonia. The absorbance of this $\delta_{\text{NH}_4^+}$ band also passed through a maximum (at approximately 730 K), which correlated well with the rate of ammonia desorption detected via mass spectrometry.

Temperature-Programmed Desorption of Ethanediamine.

The desorption rates of several characteristic products during TPD of EDA are compiled as a function of temperature in Figure 9. Table 5 compiles the maxima of the desorption rates. From HM10 EDA desorbed reactively as ammonia and hydrocarbons at temperatures above 600 K. The desorption rate of ammonia peaked at 686 K (with a shoulder at higher temperatures), while the hydrocarbons (consisting mainly of ethene and propene) showed a maximum rate of desorption at higher temperatures (727 K for ethene). Small amounts of fragments with a molecular weight exceeding that of EDA were also observed.

In contrast to HM10, a fraction of the EDA molecules sorbed on HM20 desorbed molecularly at rather low temperatures (489 K). Moreover, three maxima in the rate of desorption of ammonia were observed at 542, 596, and 695 K, instead of one in the case of HM10. The desorption of ammonia in the high-temperature desorption peak and the release of the hydrocarbon fragments from the surface were similar on HM20 and HM10.

The IR spectra recorded during TPD of EDA from HM10 are presented in Figure 10. In this experiment slightly different conditions were chosen. Adsorption prior to TPD was carried out only at 10^{-3} mbar. The coverage of Brønsted acid sites at the beginning of the TPD was 70%, and TPD was carried out with a ramp of 10 K min^{-1} . By means of mass spectrometry a molecular desorption of EDA could be observed (maximum desorption rate at 400 K). The intensity of the IR bands of the CH_2 groups decreased simultaneously. Between 325 and 560 K the intensity of all bands characteristic for NH_2 groups (ν_{NH_2} at 3363 cm^{-1} , δ_{NH_2} at 1604 cm^{-1}) decreased with increasing temperature, while the intensity of the band typical for NH_3^+ groups ($\delta_{\text{sym},\text{NH}_3^+}$ 1510 cm^{-1}) increased. Simultaneously, the small residual ν_{OH} band of free Brønsted OH groups (at 3610 cm^{-1}) disappeared completely. At temperatures higher than 560 K all infrared bands simultaneously decreased in intensity. Further changes in the shape of the spectra did not occur, only the ν_{OH} band of free Brønsted OH groups reappeared as the temperature increased.

4. Discussion

Interaction of the Mordenites with the Functional Groups of AE and EDA. Upon chemisorption of AE on the Brønsted acidic hydroxyl groups of H-mordenite the amino group is protonated and forms an ion-pair complex with the, then, negatively charged zeolite lattice (for details of the assignment compare sorption of methylamine on HM20¹¹).

For the second functional group of AE, the OH group, two different forms of interaction with the zeolite are suggested by the IR spectra. The ν_{OH} band at 3575 cm^{-1} is due to rather freely vibrating hydroxyl groups which only weakly interact with the zeolite lattice.¹⁴ The broad band between 3600 and 3350 cm^{-1} is assigned to a hydrogen-bonded species. Hydrogen bonding between the OH group of AE and lattice oxygens (see Figure 11) and intermolecular interactions between sorbed AE molecules may contribute to this band. All AE molecules sorbed on EDTA-HM10 and HM10 showed the above-mentioned strong interactions via hydrogen bonds, whereas rather freely vibrating functional groups are prominent only on HM20. A similar observation¹⁵ was also made for sorption of methanol on sodium-exchanged mordenites. Freely vibrating hydroxyl groups were found upon sorption on M20 but not on M10. This suggests that the strength of interaction between the alcoholic hydroxyl group and lattice oxygen increases with increasing framework aluminum concentration.¹⁴

For adsorption of EDA on H-mordenites one amino group of EDA is concluded to be protonated upon sorption of each molecule on the Brønsted hydroxyl groups of mordenite. Depending on energetic and geometrical factors (availability of a second acid site), the second amino group may either be protonated or only weakly interacting (ν_{NH_2} band at 3363 cm^{-1}). A comparison of the intensities of the corresponding bands (ν_{NH_2} at 3363 cm^{-1} , $\delta_{\text{NH}_3^+,\text{sym}}$ at 1510 cm^{-1}) suggests that the percentage of weakly interacting amino groups is much higher on HM20 and on EDTA-HM10 than on HM10. We suggest that the small pore volume of HM10 (see next section) leads to pore filling before a 1:1 stoichiometry of sorbed EDA molecules and Brønsted acid sites is reached. In this case both amino groups of EDA interact with the acid sites. For EDTA-HM10 and HM20, on the other hand, most EDA molecules interact only with one amino group, the other remains rather free, i.e., the situation comes closer to a 1:1 sorption stoichiometry. Moreover, physisorbed EDA contributes to the high intensity of the band of freely vibrating amino groups found for these two mordenites.

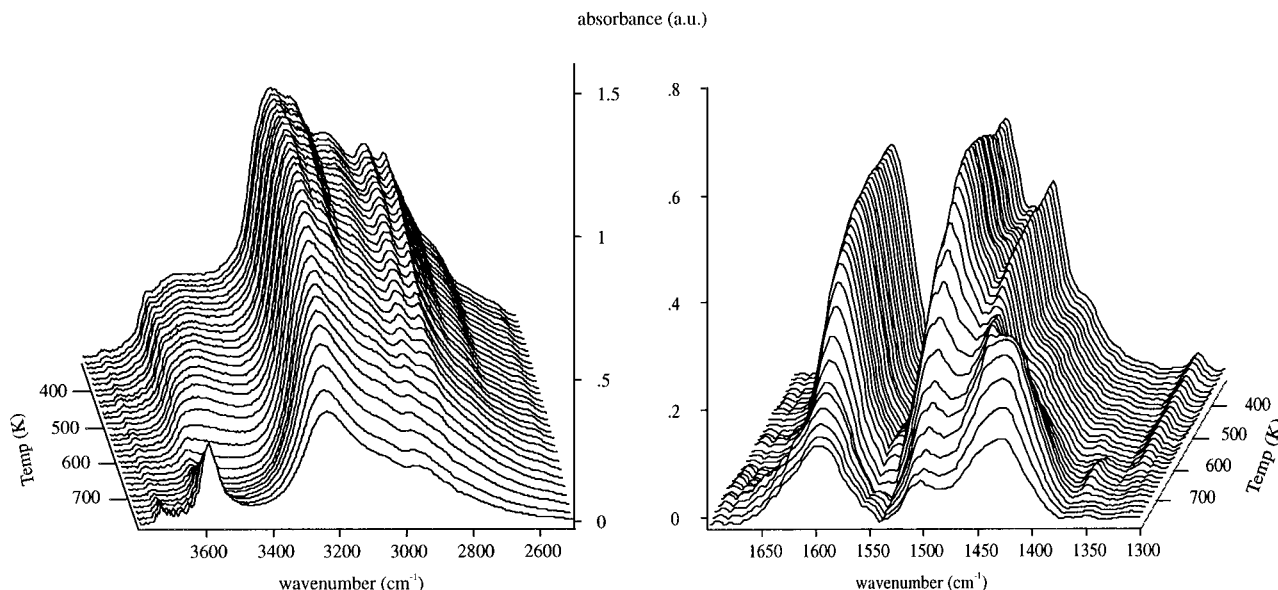


Figure 8. IR spectra of HM10 during TPD of AE. In the spectra on the right side the spectrum of activated HM10 was subtracted.

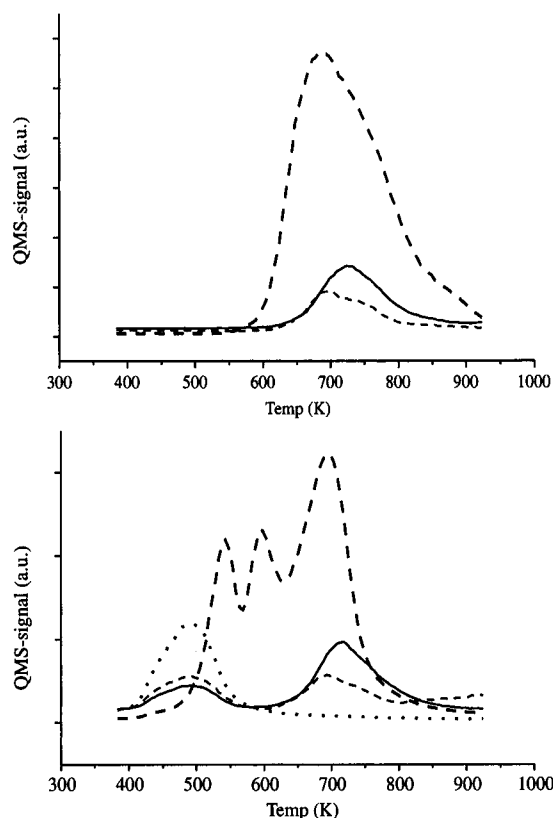


Figure 9. TPD of EDA from HM10 (a) and HM20 (b): QMS signals of mass 16 (NH_3 , ---), mass 28 (C_2H_4 , —), mass 30 (AE, ...) and mass 43 (C_3H_6 , - · -, $\times 5$).

Effect of the Pore Volume on the Sorption Properties.

Most of the differences in the sorption properties of HM10 compared to HM20 can be explained by the drastically different micropore volume of these two catalysts (0.05 vs $0.13 \text{ cm}^3/\text{g}$). Table 6 compares these properties for the three mordenites HM10, EDTA-HM10, and HM20. HM10, the sample with the smallest micropore volume, was the only of the three catalysts that did not allow a full coverage of the Brønsted acid sites. Moreover, physisorbed molecules are not present in the pores of HM10, as concluded from the absence of bands of nonprotonated amino groups in the IR spectrum of sorbed AE. Accordingly, during TPD of AE and EDA from HM10

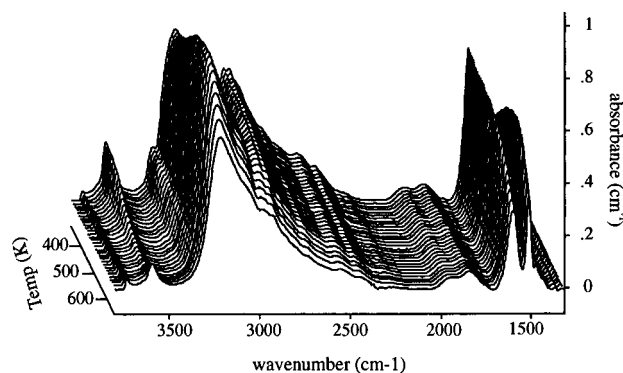


Figure 10. IR spectra of HM10 recorded during TPD of EDA.

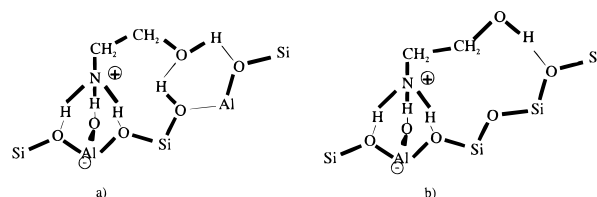


Figure 11. Possible adsorption structures of AE: (a) The amino group of AE is protonated on a Brønsted acid site. The OH group is hydrogen bonded to a neighboring acid site. (b) The amino group is protonated, the OH group is hydrogen bonded to the lattice oxygens.

TABLE 5: Temperature Maxima in the Desorption Rate during TPD of EDA from HM10 and HM20

temp (K)		assignment
HM10	HM20	
	589	EDA
	542	NH_3
	596	NH_3
686	695	NH_3
727	715	C_2H_4

desorption at low temperatures, characteristic for weakly bound (physisorbed) species, was not observed. We think that at a coverage below one molecule per site the pores of HM10 are filled and, thus, chemi- and physisorption of further molecules is impossible.

Further evidence for the severe steric restrictions in the transport and sorption on HM10 was obtained by the coadsorption experiments. The relative surface concentrations at steady

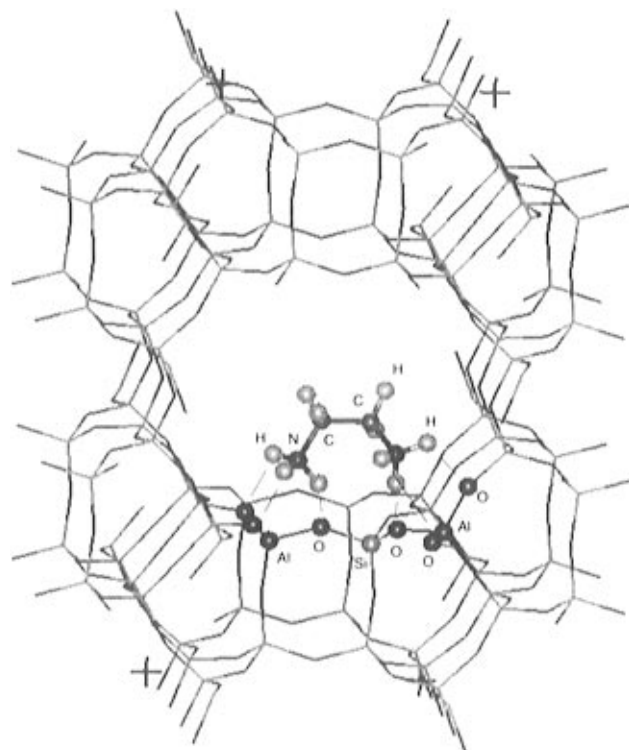


Figure 12. Graphical representation of a double protonated EDA molecule in the main channel of MOR. Printed out from Insight II molecular modeling system (Biosym/MSI, San Diego).

TABLE 6: Comparison of the Properties of the Three Mordenites That Are Related to Pore Volume

	HM10	EDTA-HM10	HM20
θ_{SiOHAl}^a	0.75–0.85	1.00	1.00
AE fully replaces ammonia	no	nd ^c	yes
physisorbed species detected in IR ^b	no	yes	yes
low-temp TPD peak	no	nd ^c	yes

^a Coverage of Brønsted acid sites at a partial pressure of 10^{-3} mbar AE and 323 K (calculated from the change in intensity of the ν_{OH} band at 3610 cm^{-1}). ^b As indicated by the presence of nonprotonated NH_2 groups upon sorption of AE. ^c Not determined.

state depend on the sequence of adsorption of the two reactants. The substance introduced first was always present as the main sorbed species. This indicates that the very slow diffusion in the pores of HM10 prevents equilibration within the time frame of the experiments. As a result, AE did not fully replace ammonia on HM10 (as expected from the basicity of the two substances), whereas it did on HM20, having the larger pore volume. The small pore volume and the severe diffusional limitations in HM10 are concluded to be due to the presence of extraframework alumina (EFAL) species partially blocking and/or filling the pores of this zeolite sample. The increase of the pore volume by a factor of 2 upon EDTA treatment and the sorption experiments showed a drastic improvement in the accessibility of the acid sites for AE and EDA. Thus, we conclude that the EDTA treatment removed most of EFAL. Although some aluminum atoms were removed from the zeolite (as indicated by the increase in the Si/Al ratio from 5.0 to 6.0) the number of Brønsted acid sites as determined by ammonia adsorption remained almost constant (see Table 1). Also the approximately identical intensity of the ν_{OH} band at 3610 cm^{-1} of HM10 and EDTA–HM10 indicates that the number of Brønsted sites does not change significantly.

Temperature-Programmed Desorption of Aminoethanol. The TPD experiments suggest that the strongly sorbed EA

molecules decompose stepwise releasing first water and then ammonia and a mixture of alkenes and alkanes. This indicates that the process is not monomolecular and invokes complex condensation and/or oligomerization steps. In this course, molecules with higher molecular weight are formed, which partly desorb, partly crack into ethene and propene and partly stay on the catalyst as coke.

The nature of the intermediate formed when AE eliminates water is difficult to deduce from the IR spectra. Segawa et al.³ suggested aziridine (ethyleneimine) as intermediate. Our present IR measurements performed in situ, however, do not confirm this. In one experiment the temperature ramp was stopped at 650 K, i.e., at a temperature at which water but not ammonia is already desorbed. Under these conditions the intermediate is assumed to be the most abundant surface structure. After keeping the catalyst at this temperature for 1 h, the IR spectrum still showed two bands for the asymmetric and symmetric deformation vibration of an NH_3^+ group instead of the one expected for protonated aziridine (R_2NH_2^+). Two new bands at 1455 and 1361 cm^{-1} were formed in this temperature region, which are concluded to be affiliated with the intermediate. While this does not allow to identify the intermediate, we conclude that it contains a protonated, primary amino group. Upon further increase in temperature the intermediate decomposes. Ammonia formed in the dissociation step remains bound to the Brønsted acid sites and desorbs at higher temperatures.

Temperature-Programmed Desorption of Ethanediamine.

IR measurements performed during TPD of EDA from HM10 show that in the temperature region between 325 and 560 K the bands characteristic for the nonprotonated amino groups (at 3360 and 1610 cm^{-1}) disappear and that the concentration of protonated amino groups increases (typical band at 1505 cm^{-1}). All Brønsted acid sites interact with sorbed molecules during these processes. This suggests that chemisorbed EDA that is protonated on one amino group chemisorbs via protonation also with the second amino group on free Brønsted acid sites. The higher mobility at elevated temperatures and the desorption of more weakly bound species¹⁶ seem to allow the molecules to overcome steric and/or geometrical barriers that prevent full double protonation at room temperature. The double-protonated species then desorbed at very high temperatures upon decomposition into ammonia and ethene (and other hydrocarbons), in a process similar to that proposed for AE.

Conclusions

Upon sorption of AE and EDA on the Brønsted hydroxy groups of H-mordenites, the NH_2 group of AE and one NH_2 group of EDA are protonated. On H-mordenites with a high aluminum concentration, the interaction of the second functional group with the zeolite is stronger than on the silicon rich samples. The OH group of AE was hydrogen bonded, and a fraction of the EDA molecules is protonated on the second amino group as well.

In experiments, when AE and ammonia were coadsorbed, preferential adsorption of AE over ammonia is observed on HM20. On HM10, the experiments indicate the formation of a bimolecular complex, in which AE and ammonia are sorbed on neighboring acid sites and interact via hydrogen bonding.

During TPD of AE from H-mordenites, the molecule eliminated water at approximately 600 K, the temperature at which the conversion of AE to EDA over mordenites is carried out.^{3,4} This supports the claim of Segawa et al.³ that elimination of water from AE is the first step in the reaction with ammonia to EDA. Higher temperatures seem to be unfavorable due to decomposition of AE into ammonia and hydrocarbons.

During TPD of EDA from H-mordenites, the increased mobility at higher temperatures enables all EDA molecules to be protonated on both amino groups. This strongly bound species then desorbs at temperatures above 600 K upon decomposition into ammonia and hydrocarbons. The TPD results indicate that desorption might be a limiting step in the catalytic conversion of AE to EDA, and we speculate that an adsorption-assisted desorption mechanism¹² is operative when sorbed EDA is replaced by incoming AE or ammonia.

Acknowledgment. Partial support of this work by NIOK is gratefully acknowledged. G.D.P. is grateful to the Vienna University of Technology for financially supporting the stay at the University of Twente.

References and Notes

- (1) Carter, R. G.; Doumaux, A. R.; Kaiser, S. W.; Umberger, P. R. *Kirk-Othmer Encyclopedia of Chemical Technology*, 4th ed.; John Wiley & Sons: New York, 1993; Vol. 8, pp 82–108.
- (2) Mercker, H. J. *Ullmann's Encyclopedia of Industrial Chemistry*, 4th ed.; VCH-Verlagsgesellschaft: Weinheim, 1985; Vol. A2, p 23.
- (3) Segawa, K.; Mizuno, S.; Maruyama, Y.; Nakata, S. *Stud. Surf. Sci. Catal.* **1994**, *84*, 1943.
- (4) Deeba, M.; Ford, M. E.; Johnson, T. A.; Premecz, J. E. *J. Mol. Catal.* **1990**, *60*, 11.
- (5) JP application 07-247245 A2, 1995.
- (6) Sawa, M.; Niwa, M.; Murakami, Y. *Zeolites* **1990**, *10*, 532.
- (7) Kogelbauer, A. Ph.D. Thesis, Vienna University of Technology, 1987, p 12.
- (8) Zhan, Zhaoqi Ph.D. Thesis, University of Twente, 1995, p 25.
- (9) Colthup, N. B.; Daly, L. H.; Wiberly, S. E. *Introduction to Infrared and Raman Spectroscopy*, 3rd ed.; Academic Press: Boston, 1990; Chapter 11.
- (10) Pouchert, Ch. J. *The Aldrich library of FT-IR spectra*, 1st ed.; Aldrich Chemical Co.: Milwaukee, WI, 1985.
- (11) Gründling, Ch. Ph.D. Thesis, University of Twente, 1995, Chapter 2.
- (12) Gründling, Ch.; Eder-Mirth, G.; Lercher, J. A. *Res. Chem. Intermed.*, in press.
- (13) Teunissen, E. H.; van Santen, R. A.; Jansen, A. P. J.; Duijneveldt, F. B. *J. Phys. Chem.* **1993**, *97*, 203.
- (14) Eder-Mirth, G.; Lercher, J. A. *Recl. Trav. Chim. Pays-Bas* **1996**, *115*, 157.
- (15) Kogelbauer, A.; Gründling, Ch.; Lercher, J. A. *J. Phys. Chem.* **1996**, *100*, 1852.
- (16) The fact that molecular desorption of EDA was not observed in the other vacuum-TPD setup may be due to readsorption effects in the deep catalyst bed.